ABSORPTION AND LUMINESCENCE EXPERIMENTS IN SEMICONDUCTOR SUPERLATTICES

M. Voos

JOURNAL DE PHYSIQUE
Colloque C5, supplément au n°4, Tome 45, avril 1984

ABSORPTION AND LUMINESCENCE EXPERIMENTS IN SEMICONDUCTOR SUPERLATTICES

M. Voos

Groupe de Physique des Solides de l'Ecole Normale Supérieure, 24 rue Lhomond, 75231 Paris Cedex 05, France*

Résumé - Nous présentons ici des résultats expérimentaux obtenus récemment à partir de mesures optiques faites sur des super-réseaux semiconducteurs. Ces études ont donné des informations intéressantes sur les propriétés électroniques de ces systèmes à deux dimensions qui ont ouvert un nouveau champ de recherche en physique des semiconducteurs.

Abstract - We present here some experimental results obtained recently on semiconductor superlattices from optical measurements. These studies give interesting informations on the electronic properties of these two-dimensional systems which have opened up a new field of investigations in semiconductor physics.

I - INTRODUCTION

Semiconductor superlattices, which have been proposed by Esaki and Tsu /1/, consist of thin alternate layers of two semiconductors which, generally, closely match in lattice constant. In these periodic structures, the thickness of the layers ranges from 10 Å to a few hundred Å about, smaller than or comparable to the electron mean free path, but larger than the interatomic spacing. Thus, the considered system is two-dimensional, at least in first approximation, and quantum effects can be expected, changing the electronic structure of the host materials and giving rise to unusual properties. The different band gaps E_g of the host semiconductors create a one-dimensional periodic potential in the z direction perpendicular to the plane of the layers. This leads to the creation of an artificial periodicity, which is longer than the atomic spacing and is superposed to the natural periodicity of the crystal. This potential causes a folding of the Brillouin zone, resulting in a series of quantized subbands in both the conduction and valence bands, as shown in Fig.1. One can consider that the carriers are confined in quantum potential wells and that their motion is quantized in the z direction, the conduction (valence) subbands such as E_1, E_2... (H_1, H_2...) lying at higher (lower) energy than the bottom (top) of the conduction (valence) band of the host semiconductor. Tunneling interactions between successive potential wells can give rise to an appreciable width of the subbands in the z direction, corresponding to a certain dispersion relation of the energy as a function of the electron wavevector k_z. Besides, the carrier motion is not quantized in the x, y plane of the layers, and each subband presents also a dispersion relation as a function of k_x and k_y which approximates that of the corresponding bulk semiconductor in most superlattices.

Two types of superlattices, I and II, have been extensively investigated. GaAs-$Al_xGa_{1-x}As$ structures correspond /2/ to type I, and the situation is schematically described in Fig.1. The GaAs conduction band edge is at lower energy than that of $Al_xGa_{1-x}As$, while its valence band edge is at higher energy than that of $Al_xGa_{1-x}As$. The GaAs layers are thus potential wells for both electrons and holes which are confined in these layers. In InAs-GaSb structures /3/, which belong to type II structures, the InAs conduction band edge lies at lower energy than the GaSb valence band edge, as schematized in Fig.2(a). The InAs and GaSb layers serve as potential wells for electrons and holes, respectively. Electrons and holes are spa-

tially separated, but photon absorption or emission are nevertheless possible because the electron and hole wavefunctions overlap. Furthermore, experimental investigations have shown /4/ recently that HgTe-CdTe superlattices, which belong at first sight to type I structures, have in fact quite different characteristics from those of GaAs-AlGaAs systems.

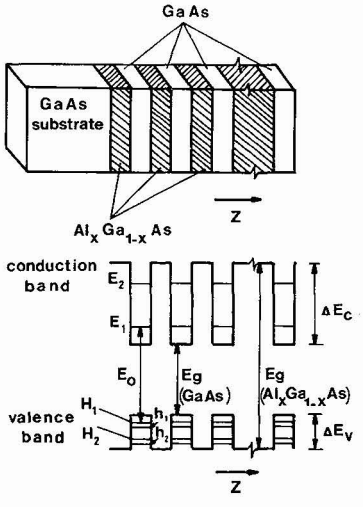

Figure 1 : Schematization of a semiconductor superlattice consisting here in alternate layers of GaAs and $Al_xGa_{1-x}As$. The total thickness of the superlattice is generally of the order of 1 µm, and that of the substrate is typically 500 µm. Also shown is the variation of the conduction and valence bands in such a structure in the z direction perpendicular to the layers. Several conduction (E_1, E_2) and valence (H_1, h_1, H_2, h_2) subbands are represented here, where H_1 and H_2 correspond to heavy-holes, while h_1 and h_2 are light-hole subbands. The superlattice band gap is $E_o = E_1 - H_1$.

In addition to the spatial separation of electron and holes, there is another important difference between GaAs-$Al_xGa_{1-x}As$ and InAs-GaSb superlattices. The electron effective mass in InAs (0.023 m_o) /5/ is much lighter than in GaAs (0.066 m_o) /5/, which leads to stronger tunneling interactions between InAs layers than between GaAs layers. Thus, in InAs-GaSb structures, even for rather large values of the layer thicknesses ($\sim$ 200 Å), the E_1 subband has /3/ an appreciable width ΔE_1 in the z direction, while ΔE_1 is often negligible in GaAs-$Al_xGa_{1-x}As$ superlattices. Furthermore, due to the large heavy-hole effective mass in III-V compounds ($\sim$ 0.3 m_o) /5/, the width of the H_1 subband in the z direction, ΔH_1, is approximately equal to zero.

It is not possible to review here all the optical studies performed on semiconductor superlattices, and we will only describe some of the results which have given interesting informations on their electronic properties. We will focus on GaAs-$Al_xGa_{1-x}As$ and InAs-GaSb superlattices, which are the most extensively investigated structures, and we will also describe briefly some aspects of HgTe-CdTe superlattices. However, it should be noted that other superlattices, such as $In_xGa_{1-x}As$-InP /6/ and GaSb-AlSb /7/ systems for example, are now being investigated.

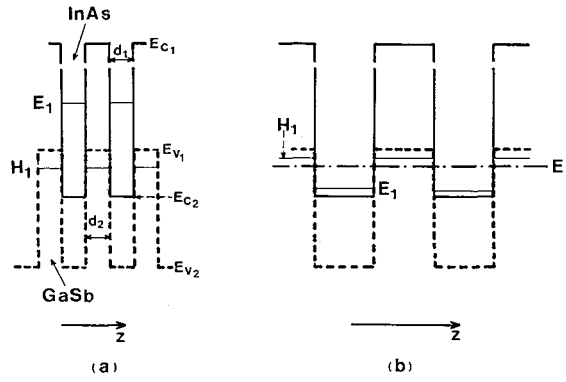

Figure 2 : Schematic energy diagram of an InAs-GaSb superlattice. E_{c1} (E_{c2}) and E_{v1} (E_{v2}) are the conduction and valence band edges of GaSb (InAs). E_1 and H_1 are respectively the ground conduction and valence subbands of the superlattice. Semiconducting (a) and semimetallic (b) situations.

II - OPTICAL ABSORPTION AND LUMINESCENCE

Absorption experiments done at helium temperatures in GaAs-$Al_xGa_{1-x}As$ superlattices grown by molecular beam epitaxy (MBE) have given strong evidence for carrier confinement in the GaAs potential wells /2,8/. Typical data are shown in Fig.3 which presents transmission (i.e. absorption) and excitation spectra /8/. Excitation spectroscopy, which gives the same informations as optical absorption, consist in scanning the exciting light wavelength from a dye laser while the detecting spectrometer is set at an energy where the sample exhibits luminescence, i.e. here at 1.525 eV (see Fig.3). Peaks are found at energies corresponding to possible transitions shown in the inset of Fig.3 as a result of photon absorption by the corresponding energy levels followed by rapid relaxation of the excited carriers to the luminescent level where they recombine radiatively. In fact, the peaks in Figs 3(b) and 3(c) are characteristic of light absorption by free excitons /2/, and, the observed optical transitions are identified in Fig.3 where the n = 1e - hh peak, for instance, is attributed to absorption by a free exciton corresponding to the n = 1 electron (E_1 subband) and heavy-hole (H_1 subband) states shown in the inset. Carrier confinement is clearly observed since, in bulk GaAs, the absorption spectrum presents /2/ only a free exciton peak at 1.515 eV, namely at lower energy than the transitions studied here. The energy position of the peaks in Fig.3 is in good agreement with calculations of the conduction and valence subband energies performed in a simple model where the GaAs layers correspond to non-interacting quantum wells having a finite depth /2/. Additional absorption experiments /2/ in similar superlattices demonstrate that, when the GaAs layer thickness is decreased, the free exciton peaks move to higher energies and the distance between these peaks increases, as can be expected in a simple quantum well model. From such investigations, the discontinuity ΔE_c (ΔE_v) of the conduction (valence) band at each interface has been found /2/ to be equal to 225 meV (30 meV) for $x \sim 0.2$. This was obtained by fitting the energy positions of the observed transitions in several superlattices having different GaAs layer thicknesses to simple calculations corresponding again to non-interacting quantum wells of finite depths /2/. More sophisticated theoretical investigations in the envelope function approximation /9/ of the superlattice band structure provides, in fact, similar results. Luminescence experiments have also been performed in superlattices grown by MBE /8/ and by metalorganic chemical vapor

deposition /10/. Fig.3(a) gives typical results obtained /8/ in the same structure as the one used in the absorption experiments described previously. From the absorption and excitation spectra, the two luminescence lines in Fig.3(a) are assigned to the recombination of free excitons involving the n = 1 electron state and the n = 1 heavy and light-hole states, respectively. It is noteworthy that, in such structures where the impurity density is low ($N_A - N_D \sim 10^{14} - 10^{15}$ cm^{-3}), the luminescence spectrum does not show intense lines involving impurities while, in bulk GaAs with a similar impurity concentration, it is dominated /11/ by extrinsic recombination peaks, but this difference with bulk GaAs is not understood.

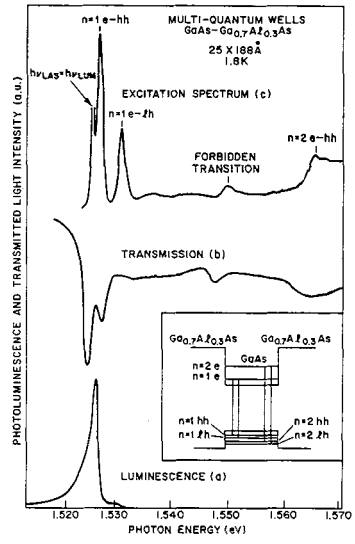

Figure 3 : Luminescence (a), absorption (b) and excitation spectra (c) of a GaAs-$Al_{0.3}Ga_{0.7}As$ superlattice consisting of 25 GaAs layers whose thickness is 188 Å, while that of the $Al_{0.3}Ga_{0.7}As$ layers is 19 Å. In the inset are shown possible optical transitions in such a structure. Here n = 1e, 2e corresponds to the E_1, E_2 subbbands, and n = 1 hh, 2 hh, 1 lh, 2 lh correspond to the H_1, H_2, h_1 and h_2 subbands shown in Fig.1. In such a structure, optical transitions are allowed for $\Delta n = 0$. (After Ref.8).

Optical absorption experiments have been done in MBE-grown InAs-GaSb superlattices /12/ for layer thicknesses ranging from 15 to 30 Å about. They give evidence for the existence of a superlattice structure, but no free exciton transitions have been observed, which is not surprising because the spatial separation of electrons and holes is not favorable to the formation of free excitons /9/. The absorption edge, which is found to depend on the layer thickness, determines the superlattice band gap $E_o = E_1 - H_1$. By comparing these data to the theoretical variation of E_o with the layer thickness calculated by the LCAO method /13/, one obtains $E_s \sim 150$ meV, where E_s is the difference between the InAs conduction band edge and the GaSb valence band edge at each interface. Besides, luminescence experiments have been performed in InAs-GaSb superlattices /14/ where the InAs and GaSb layer thicknesses were respectively d_1 = 30 Å and d_2 = 50 Å. The observed spectra, which are shown in Fig.4, lie around 250 meV, and are therefore at much lower energy than the band gaps /5/ of bulk InAs (410 meV) and GaSb (815 meV), indicating the formation of subbands in the superlattice. In this system, LCAO calculations of the superlattice band structure /13,15/ give ΔE_1 = 60 meV, while $\Delta H_1 \sim 0$. Therefore, the hole density of states is actually two-dimensional, but that of electrons is not strictly two-dimensional as a result of the non-zero width of E_1. Taking into account the actual electron and hole densities of states, as well as the calculated optical matrix element which, in these structures, depends /16/ on k_z, theoretical fits of the main line in Fig.4 show that it is due, over the whole temperature range investigated, to band-to-band recombination between free electrons in the E_1 subband and free holes

in the H_1 subband. In addition, the superlattice band gap, E_o, obtained at 2 K from such a fit is equal to 262 meV, in satisfying agreement with the theoretical value /9,13/ (280 meV). As can be seen in Fig.4, when T is reduced below 300 K, the luminescence spectrum exhibits a tail or a bump on its low-energy side which indicates the existence of energy states in the superlattice band gap. They may correspond to impurities whose behavior in superlattices has been studied theoretically by Bastard /17/. They may also arise /14/, as observed in GaAs-Al_xGa_{1-x} systems /18/, from interface defects looking like surface roughness and corresponding to thickness fluctuations within each layer. However, at this stage, it does not seem possible to determine which processes are responsible for this low-energy tail.

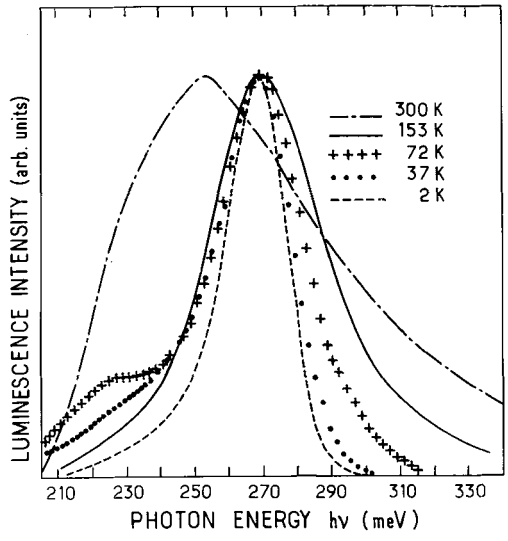

Figure 4 : Luminescence spectra observed in an InAs-GaSb superlattice at different temperatures. (After Ref.14).

III - MAGNETO-ABSORPTION EXPERIMENTS

At first, it is important to note that Esaki et al. have suggested /3,13/ that a semiconductor-semimetal transition should take place in InAs-GaSb superlattices when the layer thickness becomes of the order of 100 Å. When the layer thickness is smaller than 100 Å (Fig.2(a)), the E_1 subband, mainly localized in the InAs layers, is at higher energy than the H_1 subband, which is confined in the GaSb layers. Therefore, the superlattice band gap, $E_o = E_1 - H_1$, is positive and corresponds to a semiconducting situation which was studied in the previous section. When the layer thickness is increased, E_1 is lowered and H_1 is raised, in first approximation as in a simple quantum well. When the layer thickenss is larger than 100 Å about, H_1 is at higher energy than E_1 and $E_1 - H_1$ is negative (Fig.2(b)), the corresponding structure being semimetallic. In such a simple model /19/, electrons transfer from H_1 to E_1, namely from GaSb to InAs layers, and the Fermi level, E_F, lies between E_1 and H_1, close to H_1 because of the large heavy-hole mass.

Interesting informations have been obtained from far-infrared (FIR) magneto-absorption experiments /20-22/ performed in MBE-grown InAs-GaSb superlattices (S1, S2) whose InAs and GaSb thicknesses are given in Table I. In these experiments the far-infrared transmission of these samples was studied at fixed photon energies as a function of the magnetic field B, which was perpendicular to the plane of the layers, the infrared radiation being near normal incidence to the layers. Figure 5 gives typical transmission spectra in sample S1, showing that the transmission signal versus B exhibits pronounced oscillations. In Fig.6 are shown, as a function of B, the infrared photon energy positions of the transmission minima (i.e. absorp-

tion maxima) obtained from the observed oscillations (Fig.5).

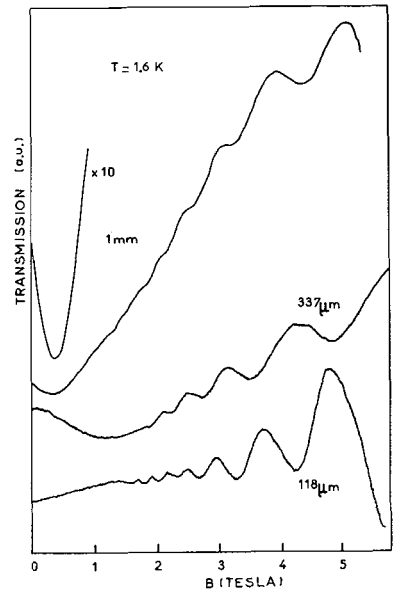

Figure 5 : Transmission spectra versus B for different infrared wavelengths. (After Ref.20).

As can be deduced from simple theoretical analyses /20-22/, the photon energies, $h\nu$, at which these minima occur depend almost linearly on B. Extrapolation to B = 0 results in $h\nu = 0$ for the line noted CR, $h\nu = -39$ meV for the lines labelled 1, 2, 3..., and $h\nu = -16$ meV for the line noted 0'. The CR line (Fig.6) is attributed to electron cyclotron resonance, i.e. to transitions from the last filled to the first empty Landau level of E_1. The curves converging to $h\nu = -39$ meV are assigned to interband transitions from H_1 to E_1 Landau levels at $k_z = 0$. The line 0' is associated to similar interband transitions occuring at the superlattice Brillouin zone boundary i.e. at $k_z = \pi/d$, where d is the superlattice periodicity. These interband transitions are represented in Fig.7(a) which gives the band structure of a superlattice along k_z with and without magnetic field in the semimetallic model. As mentioned previously, the E_1 subband, which is below H_1, has a finite width ΔE_1, but that of H_1 is essentially zero. Under a magnetic field, E_1 and H_1 exhibit both a series of Landau levels moving upward and downward, respectively, when B is increased. It is clear that each Landau level of H_1 should give rise to a single peak in the density of states (Fig.7(b)). However, E_1 is flat at $k_z = 0$ and $k_z = \pi/d$, so that there should be two peaks in the corresponding density of states for each Landau level. If the selection rules for interband transitions are taken to be $\Delta k_z = 0$ and $\Delta N = 0$, where N is the Landau index, two sets of transitions can be expected, at $k_z = 0$ and π/d, respectively, as schematized in Fig.7(a), where the interband transitions at $k_z = 0$ are noted 1, 2 and those occuring at $k_z = \pi/d$ are labelled 0', 1'.

The Landau levels $E_{1,N}$ and $H_{1,N}$ of E_1 and H_1, respectively, can be calculated using a simple theoretical model /19-22/. To obtain $E_{1,N}$, the InAs conduction band nonparabolicity is taken into account on the basis of the simplified version of the Kane model /19-22/, leading to the following relation :

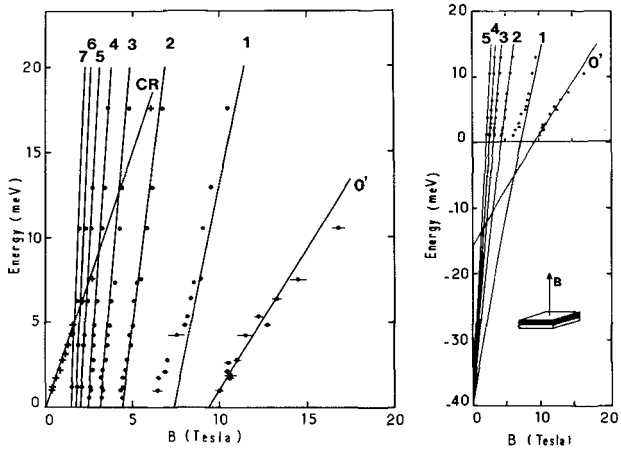

Figure 6 : Position of the transmission minima as a function of the infrared photon energy and B (+,•). The solid lines correspond to theoretical fits as described in the text. The curves noted 1,2... correspond to transitions at $k_z = 0$ from H_1 Landau levels up to E_1 Landau levels with the same Landau index, i.e. N = 1,2...; the one noted 0' corresponds to similar transitions at $k_z = \pi/d$ with N = 0. The inset shows schematically the geometry of the experiment. (After Ref.21).

$$E_{1,N} = -\frac{1}{2} E_g + \left[\frac{1}{2} (E_g)^2 + E_g D_N\right]^{1/2} \qquad (1)$$

where E_g is the band gap of bulk InAs and is equal /5/ to 410 meV. D_N is given by :

$$D_N = (N + 1/2) \hbar\omega_c + E_1 (1 + E_1/E_g) \qquad (2)$$

Here $\omega_c = e B/m_e^*$ is the electron cyclotron frequency in bulk InAs, m_e^* being its band edge mass equal /5/ to 0.023 m_o. Besides, all the energies are measured from the conduction band edge of bulk InAs. Furthermore, $H_{1,N} = H_1 - (N + 1/2) \hbar\omega_v$, with $\omega_v = e B/m_v^*$ where $m_v^* = 0.33\ m_o$ is the GaSb heavy-hole effective mass /5/.

For CR transitions, $h\nu = E_{1,N+1} - E_{1,N}$, N being such that E_F is between $E_{1,N}$ and $E_{1,N+1}$. For interband transitions at $k_z = 0$, $h\nu = E_{1,N} - H_{1,N}$ with the previous selection rules. Fits of the experimental data to this simple model are presented in Fig.6 and give the values of E_1 and H_1 at B = 0 which are listed in Table 1 for samples S1 and S2. Also given in Table 1 is the superlattice electron mass m^* which has been determined from the CR data. It is clear that m^* is larger than the band edge mass of bulk InAs, and it has been shown /20/ that this is due to the InAs conduction band non-parabolicity. This demonstrates that electrons are actually confined in the InAs layers. In addition, it should be noted that $E_1 - H_1$ is negative, as expected in a semimetallic situation. Using the same model, the interband transitions at $k_z = \pi/d$ can be also calculated, replacing E_1 by $E_1 + \Delta E_1$ in Eq.2. In Fig.6 are presented theoretical fits of the data for N = 0'. They yield ΔE_1 at B = 0 whose value, obtained /21,22/ from these studies, is given in Table 1 for both samples. Table 1 gives also the values of E_1, H_1 and ΔE_1 calculated by the LCAO method /13,15/ showing that the experimental and theoretical results compare favorably in both samples.

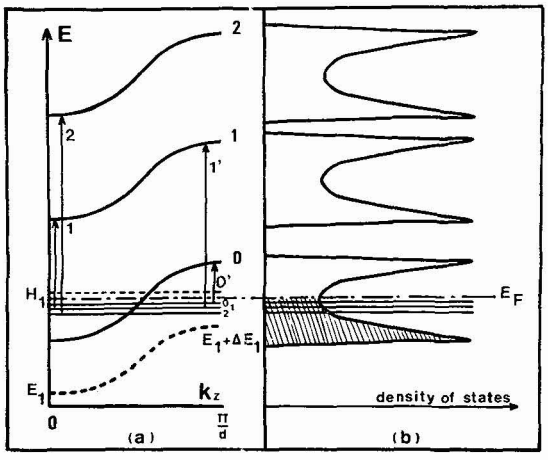

Figure 7 : (a) Schematic band structure of a semimetallic InAs-GaSb superlattice along k_z . The dashed curves are without magnetic field, the solid curves are the corresponding Landau levels under magnetic field, and E_F is the Fermi level. The transitions shown here correspond to those defined in the text and the caption of Fig.6. (b) Density of states associated with the E_1 and H_1 subbands under magnetic field. The hatched area corresponds to states occupied by electrons. (After Ref.21).

Samples	d_1 (Å)	d_2 (Å)	Theory (LCAO)			Experiment			
			E_1 (meV)	ΔE_1 (meV)	H_1 (meV)	E_1 (meV)	ΔE_1 (meV)	H_1 (meV)	m^*/m_o
S1	120	80	94	19	132	100±15	23±1	139±15	0.0385
S2	200	100	68	15	140	70±10	19±1	128±10	0.0375

Table 1 : Thickness of the InAs (d_1) and GaSb (d_2) layers for samples S1 and S2. The experimental and theoretical values of E_1, H_1 and ΔE_1, and the measured electron cyclotron mass m^* are also shown here.

The observation of a negative energy gap is consistent with the proposed semimetallic nature of these superlattices /3,13/, and these studies have provided the first experimental determination in these structures of the subband energies E_1 and H_1, and also of ΔE_1. In addition, the measurement of ΔE_1 demonstrates that the electron system in such InAs-GaSb superlattices exhibits a three-dimensional character, deviating therefore from the strict two-dimensionality corresponding to uncoupled quantum wells. Finally, it is perhaps worth mentioning that similar experiments done in semiconducting InAs-GaSb superlattices exhibit only transitions due to cyclotron resonance.

Similar far-infrared magneto-absorption experiments have been done /4/ recently at 1.6 K in a MBE grown HgTe-CdTe superlattice consisting of 200 alternate layers of HgTe and CdTe whose thicknesses are 180 and 44 A, respectively. The data have also been interpreted in terms of interband transitions from valence to conduction sub-

bands, and from these investigations it has been possible to deduce the superlattice band structure along the growth axis. This band structure is shown in Fig.8(b), that of bulk HgTe and CdTe being represented in Fig.8(a). These studies show, in particular, that the considered structure is a quasi-zero energy gap semiconductor, and provide the first determination of the offset Λ between the HgTe and CdTe valence bands which is $\sim$ 40 meV.

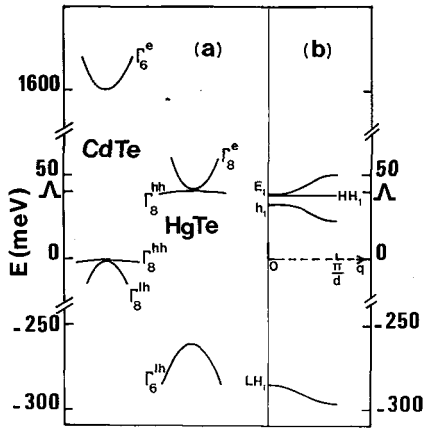

Figure 8 : (a) Band structure of bulk HgTe and CdTe.
(b) Band structure along the growth axis of the HgTe-CdTe superlattice investigated in Ref.4. E_1, HH_1, and h_1 are the ground conduction, heavy-hole and light-hole subbands. LH_1 is a light-hole subband derived from the Γ_6^{lh} HgTe states. (After Ref.4).

IV - CONCLUSION

This short review is certainly not exhaustive, but describes briefly some optical studies which have been helpful to understand the electronic properties of semiconductor superlattices. By choosing the host semiconductors and the layer thicknesses, it is clear that one can grow a tailor-made material with a band structure quite different from that of the basis semiconductors. One can certainly consider that these systems, together with modulation-doped heterojunctions, constitute a new class of two-dimensional systems which has opened up a very active and important field of research in semiconductor physics.

ACKNOWLEDGEMENTS

The author would like to thank L.L. Chang and L. Esaki from IBM and also J.P. Faurie and A. Million from LIR-LETI (Grenoble) for helpful discussions and the supply of the InAs-GaSb (IBM) and HgTe-CdTe (LIR-LETI) superlattices investigated in his laboratory. He wishes also to thank his colleagues, G. Bastard, Y. Guldner, J.P. Vieren and P. Voisin who participated very closely to the studies performed on these structures at the Groupe de Physique des Solides de l'E.N.S. He wants, also to acknowledge the efficient and kind collaboration of J.C. Maan from the MPI in Grenoble where high-magnetic field experiments on InAs-GaSb superlattices were done.

REFERENCES

*Laboratoire associé au C.N.R.S.

1. Esaki L. and Tsu R., IBM J. Res. Develop. 14 (1970) 61.
2. See, for example, Dingle R., in Festköperprobleme (Advances in Physics), ed. by H.J. Queisser (Pergamon-Vieweg, Braunschweig, 1975), Vol.15, p.21.
3. See, for example, Esaki L. and Chang L.L., J. Magn. Magn. Mater. 11 (1979) 208.
4. Guldner Y., Bastard G., Vieren J.P., Voos M., Faurie J.P. and Million A., 5th International Conference on the Electronic Properties of Two Dimensional Systems, Oxford, United Kingdom, 1983, to be published.
5. Handbook of Electronic Materials, ed. by M. Neuberger (Plenum, New York, 1971), Vol.2.
6. Voos M., J. Vac. Sci. Technol. B1 (1983) 404.
7. Voisin P., Bastard G., Voos M., Mendez E.E., Chang C.A., Chang L.L. and Esaki L., J. Vac. Sci. Technol. B1 (1983) 409.
8. Weisbuch C., Miller R.C., Dingle R. and Gossard A.C., Sol. St. Commun. 37 (1981) 219.
9. Bastard G., in Proceedings of the NATO School on MBE and Heterostructures, Erice, Italy, 1983 (Martinus Nijhoff Publishers, The Netherlands), to be published.
10. See, for example, Frijlink P.M. and Maluenda J., Jap. J. Appl. Phys. 21 (1982) L 574.
11. See, for example, Weisbuch C., Thesis, Université Paris VII (1977).
12. Sai-Halasz G.A., Chang L.L., Welter J.M., Chang C.A. and Esaki L., Sol. St. Commun. 27 (1978) 935.
13. Sai-Halasz G.A., Esaki L. and Harrison W., Phys. Rev. B18 (1978) 2812.
14. Voisin P., Bastard G., Gonçalvès da Silva C.E.T., Voos M., Chang L.L. and Esaki L., Sol. St. Commun. 39 (1981) 79.
15. Calculations done in the envelope function approximation give in fact quite similar results. See Bastard G., Ref.9.
16. Voisin P., Bastard G. and Voos M., Phys. Rev., to be published.
17. Bastard G., Phys. Rev. B24 (1981) 4714.
18. See, for example, Petroff P.M., Gossard A.C., Wiegmann W. and Savage A., J. Crystal Growth 44 (1978) 5.
19. For a detailed discussion, see Voisin P., Thesis, University of Paris-Sud, Orsay (1983).
20. Guldner Y., Vieren J.P., Voisin P., Voos M., Chang L.L. and Esaki L., Phys. Rev. Lett. 45 (1980) 1719.
21. Maan J.C., Guldner Y., Vieren J.P., Voisin P., Voos M., Chang L.L. and Esaki L., Sol. St. Commun. 39 (1981) 689.
22. Voos M., Surface Sci. 113 (1982) 94.